American Mineralogist, Volume 85, pages 868–872, 2000

Determination of water contents of granite melt inclusions by confocal laser Raman microprobe spectroscopy

R. THOMAS

GeoForschungsZentrum Potsdam, Telegrafenberg B120, D-14473 Potsdam, Germany

ABSTRACT

A new method of determining the water content of melt inclusions using confocal laser Raman microprobe spectroscopy is described. The water content of melt inclusions can be determined in the concentration range of 0 to 20 wt% with a high spatial resolution (~2 μm). Because the method works in reflection, minimal sample preparation is necessary. The method is fast, has good accuracy and precision (±0.25 wt%), and has the potential to become a useful, high resolution spectroscopic tool for melt inclusion studies.

INTRODUCTION

Water is the most important magmatic volatile. Therefore, knowledge about the evolution of water contents of melt during magma fractionation processes is key to understanding the behavior of volatiles in silicate melts. Melt inclusions provide the best available samples of volatiles in silicate melts. Hence, valid determinations of volatile constituents is possibly the most significant and useful information obtainable from silicate-melt inclusions (Roedder 1984; p. 484). For this, a simple and precise analytical method is desired. Several analytical techniques have been proposed for the determination of H_2O in silicate melt inclusions: vacuum extraction, electron microprobe analysis (EMPA), ion microprobe analysis (SIMS), and vibrational spectroscopy including Fourier transform infrared (FTIR) and Raman spectroscopy. A concise description of each technique along with a discussion of their advantages and disadvantages are given by Ihinger et al. (1994). Most of these methods are easily applied to large melt inclusions in minerals such as quartz, feldspar, and topaz from extrusive rocks with low to moderate water contents. However, for analysis of melt inclusions in minerals from intrusive rocks there are some limitations: inclusions are often smaller than 30 μm in diameter and therefore difficult to analyze by SIMS methods. Furthermore, melt inclusions from intrusive rocks often crystallize daughter crystals during cooling, so the inclusions must be rehomogenized and quenched to a homogeneous glass before analysis. FTIR spectroscopy has the disadvantage that during the rehomogenization procedure the mineral host of the inclusions becomes brittle and it is difficult or impossible to prepare doubly polished thin sections for FTIR measurements. The SIMS method may fail at high water concentrations above about 10 wt% in glasses of granitic to pegmatitic composition because of the dominance of mobile molecular H_2O (see also Ihinger et al. 1994). In contrast, micro-Raman spectroscopy has proved extremely useful for samples of only a few micrometers in size (see McMillan and Hofmeister 1988). Chabiron et al. (1999) developed a quantitative application of confocal micro-Raman spetrometry in order to determine the water contents of individual melt inclusions in a rapid and non-destructive way. This paper shows that water concentrations in quenched melt inclusions can be accurately determined even in very small inclusions having diameters as small as 3 μm over the entire concentration range of interest (0 to 20 wt% H_2O).

EXPERIMENTAL AND ANALYTICAL DETAILS

A Dilor XY Laser Raman Triple 800 mm spectrometer equipped with an Olympus optical microscope and a long distance 80× objective was used. Spectra were collected with a Peltier cooled CCD detector. The 514 nm line of a Coherent Ar^+ Laser Model Innova 70-3 and a power of 150 mW of the argon laser were used for sample excitation. The confocal technique provides an efficient way to obtain interference-free Raman spectra of small specimens embedded in a transparent matrix. The derived empirical calibration curves for determining water concentrations are only applicable to the instrument used in this study. A similar calibration procedure is necessary for each particular instrument.

Figure 1 shows the Raman spectrum of a H_2O-rich pegmatite glass collected at room temperature. The low-frequency region is characterized by an asymmetric broad band in the 490 cm^{-1} region which predominantly results from oxygen motions in the T-O-T symmetric stretching mode, where T represents tetrahedrally coordinated Si or Al (see Matson et al. 1986; Sharma et al. 1997). Additional bands in the low-frequency region include symmetric bands near 800 and 920 cm^{-1}, and a broad asymmetric band at 1100 cm^{-1} with a shoulder toward lower frequency at about 1020 cm^{-1}. According to Mysen et al. (1997), appearance of the strong band near 900 cm^{-1} results from increasing amounts of H_2O in the glasses.

The H-O-H bending vibration of molecular H_2O dissolved in the glass is indicated by the presence of a weak peak near 1630 cm^{-1} (see McMillan 1994). However, a relationship between the total water content in glass, the intensity of this peak, and the observed shift of the peak position ($\Delta \sim 30$ cm^{-1}) could

*E-mail: thomas@gfz-potsdam.de

0003-004X/00/0506–868$05.00

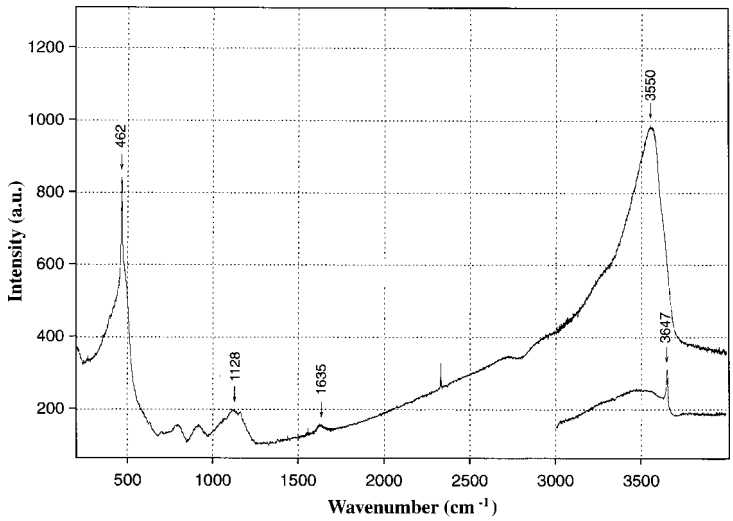

FIGURE 1. Raman spectrum of a melt inclusion in pegmatite quartz from Ehrenfriedersdorf-Erzgebirge. The inclusion was rehomogenized at a temperature of 650 °C and a pressure of 1 kbar using the conventional hydrothermal rapid-quench technique. The run duration was 96 hours. The water content of the glass is 10 wt%. The partial spectrum on the right side shows the changed intensity and the new formed band near 3650 cm^{-1} after heat treatment of an identical inclusion.

not be positively established. According to Stolper (1982) this discrepancy is most probably due to the relative insensitivity of Raman spectroscopy for detection of molecular water. The high-frequency region (3000–4000 cm^{-1}) of the unpolarized Raman spectrum is characterized by an asymmetric OH stretch band centered at 3550 cm^{-1} with a tail to lower frequencies, an obvious broad shoulder maximized near 3290 cm^{-1}, and typically a shoulder or sharp band at 3630 cm^{-1} (Fig. 1). The breadth and asymmetry of the band at 3550 cm^{-1} reflects contributions from both molecular water and other OH-containing species (Pandya et al. 1992). Gaussian deconvolution (e.g., Mysen et al. 1997) reveals that this peak may be the result of three main bands at 3350, 3500, and 3575 cm^{-1}, and an additional weak band around 3640 cm^{-1}. The presence of a weak 3640 cm^{-1} band was confirmed in spectra collected from silica glasses having high water contents (i.e., > 10 wt%). At very high bulk water contents (> 20 wt%) molecular H_2O becomes the most dominant species as shown by a shift of the very strong main band in the direction of the molecular water position ν1 (see Ihinger et al. 1994) now centered at 3450 cm^{-1}. This is shown in the spectra in Figure 2 obtained from a 4-phase melt inclusion containing two silicate melts, a fluid phase and a vapor bubble (see Thomas et al. 2000). The composition of such an extremely H_2O-rich silicate melt is given below. In this case the Raman spectrum is also characterized by a strong peak centered at 1642 cm^{-1}.

There are two methods for water determination in glass with the micro-Raman spectrometry. Both methods work in reflection and can be applied to very small sample volumes depending on the optical characteristics of the spectrometer.

In the first method, the linear relationship between the H_2O content of silicate glass and the intensity of the asymmetric OH stretch band centered at 3550 cm^{-1} is utilized (see also Stolper 1982). The intensity at the 3550 cm^{-1} position was analyzed with a single spectral window. The acquisition time was 200 s, and 3 accumulations were used in each case. The baseline correction was performed with a first-degree polynomal. With this method, the peak height was used instead of the peak area, because a larger scattering of the integral intensity with H_2O-concentration was observed during the calibration procedure. This may be a result of the strong asymmetry of the 3550 cm^{-1} band (see Fig. 1) caused by contributions from a number of species (e.g., OH, Si-OH, Al-OH, H_2O, etc.). These species may have different cross-sections which could lead to more scatter in the integral intensity of the fundamental OH-stretching peak at ~3550 cm^{-1} (see Pandya et al. 1992). Before and after each measurement, the optical configuration was verified using a large, totally homogenized melt inclusion of known H_2O content (10 wt%) as a standard. Verifying the intensities is important, because it is necessary to use exactly the same experimental conditions for all H_2O determinations. A variation of the intensity of 2.3% (1σ) as the relative standard deviation was obtained from 25 measurements at different focal depths in the standard melt inclusion.

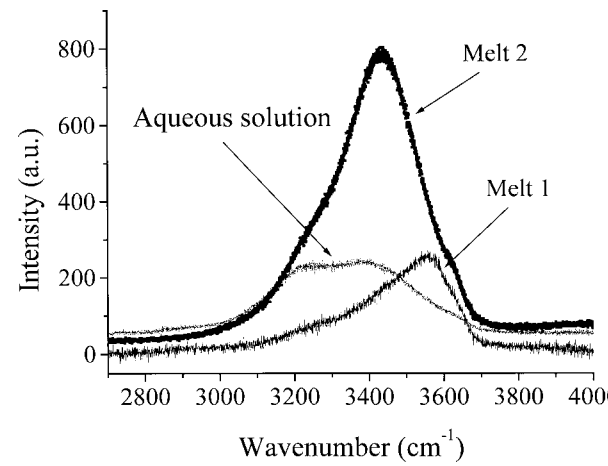

FIGURE 2. Three Raman spectra from a silicate melt inclusion in pegmatite quartz: melt 1 (silicate-rich, water-poor melt), melt 2 (water-rich silicate melt), and an aqueous solution.

In the second method, the ratio of the 3550 cm^{-1} band intensity and the intensity at 490 cm^{-1} attributed to a delocalized vibrational mode involving the symmetric stretching of bridging O atoms in T-O-T linkages (Matson at al. 1986) is used. Applying the ratio method eliminates sampling problems and reduces systematic errors and irreproducible instrumental variations. Integral intensities rather than peak heights were used. Furthermore, different counting times were applied to different samples having different water contents; 60 s for concentrations >1 wt% H_2O, and 600 s for values <1 wt% H_2O. Two spectra must be taken at different spectrometer positions for each measurement: One in the low frequency range at 490 cm^{-1} and the other in the high-frequency range at 3550 cm^{-1}, respectively. A disadvantage of this method is the increased mechanical wear to the spectrometer drive mechanism. According to Cooney et al. (1994) the problems with the mechanical setting of the spectrometer can be overcome by using two different lines of the Ar-ion laser as excitation sources: the 514.5 nm line for the low frequency region (200–1500 cm^{-1}) and the 457.9 nm laser line for the high frequency region (2631–3931 cm^{-1}). In this way, simple re-tuning of the laser enabled us to measure the both Raman spectra of the low-frequency lattice modes and the high frequency O-H stretching modes without changing the position of the laser spot or the mechanical setting of the spectrometer.

At standard conditions, the beam diameter is about 2 μm which produces an excitation volume in the range of 10 μm^3. The highest quality spectra are obtained from an excitation volume that is near the polished surface of the melt inclusion. The Raman signal from depths >10 μm beneath the surface is significantly reduced and a correction procedure must be applied. In this study only melt inclusions truncated by the polished surface (depth ≤10 μm) were selected for analyses. For inclusions near the surface of the host mineral (between 10 and 100 μm depth) a linear correction function was derived, which gives the percentage weakening of the Raman intensity with depth. Water determinations were made using both analytical methods.

RESULTS AND DISCUSSION

Raman peak intensities for water were calibrated using 26 synthetic and natural glass samples of known composition in the range between 0 and 16 wt% H_2O. Water contents of the reference samples were initially determined directly by Karl Fischer titration (KF) and indirectly by subtracting the oxide sum (in wt%) of EMPA analysis from 100% (see Thomas and Klemm 1997). The water contents of two samples was also estimated by SIMS measurements. In the case of very high water contents (>16 wt%) in pegmatitic melt inclusions in quartz, only electron microprobe analysis was effective. The samples and the results obtained from the calibration for water are given in Table 1 and are shown in Figure 3. Each datum in Table 1 is the mean of at least 10 determinations (±1σ standard deviation). In some cases, such as albite glass AB84, up to 70 deter-

TABLE 1. Raman spectrometric analyses of synthetic glasses and silicate melt inclusions

Reference glasses (Origin)	Water content, analyzed by KF (wt%)	Amplitude at ~3550 cm^{-1}	Water content Method I (wt%)	$I\left(\frac{3550\ cm^{-1}}{490\ cm^{-1}}\right)$	Water content Method II (wt%)
Piezoelectric quartz	0	0	0	–0.015 ± 0.002	(0.12)
PCD (Westrich, H. R.)	0.12	n.d.	n.d.	0.014	0.21
Albite glass (Holtz, F.)	0.65	n.d.	n.d.	0.1	0.50
N (Westrich, H. R.)	0.92	n.d.	n.d.	0.22 ± 0.02	0.93 ± 0.07
WOR40S7 (Behrens, H.	1.31 ± 0.15	36.9	1.62	0.26 ± 0.02	1.08 ± 0.08
AOQ (Holtz, F.)	1.86	41.1 ± 2.0	1.79 ± 0.08	0.43 ± 0.01	1.76 ± 0.04
2N (Westrich, H. R.)	2.02	46.4 ± 3.1	2.00 ± 0.12	0.61	2.56
WAOQ068 (Behrens, H.)	2.45	60.3	2.56	0.57 ± 0.07	2.38 ± 0.32
Albite glass Ab75 (Holtz, F.)	2.62	60.9	2.59	0.54	2.24
Albite glass Ab50 (Holtz, F.)	2.82	67.4	2.85	0.72 ± 0.03	3.08 ± 0.15
Albite glass Ab (Holtz, F.)	2.87	62.6	2.66	0.67	2.84
M3N (Westrich, H. R.)	2.95	69.2 ± 3.4	2.92 ± 0.14	0.76	3.28
Qu8-melt inclusion (Webster; J.D.)	4.3 ± 0.38*	n.d.	n.d.	0.96 ± 0.06	4.31 ± 0.32
M6N (Westrich, H. R.)	5.11	120 ± 3.0	4.97 ± 0.12	1.09 ± 0.1	5.03 ± 0.57
Leucogranite GB (Holtz, F.)	5.22 ± 0.30	126.4 ± 2.8	5.23 ± 0.12	1.03	4.70
WAB079 (Behrens, H.)	5.92 ± 0.15	138.4 ± 2.5	5.72 ± 0.10	1.26 ± 0.01	6.03 ± 0.06
Haplogranite 1.2 (Holtz, F.)	6.13	147.1	6.07	1.37 ± 0.04	6.72 ± 0.25
WOR100S7 (Behrens, H.)	6.54 ± 0.15	157.8	6.50	1.28	6.16
Qu8-melt inclusion (Webster; J.D.)	6.90 ± 0.38*	n.d.	n.d.	1.41 ± 0.05	6.97 ± 0.32
WAOQ31 (Behrens, H.)	7.81	n.d.	n.d.	1.56 ± 0.09	7.96 ± 0.61
Leucogranite GB (Holtz, F.) - 1	8.36	205.7	8.43	1.61 ± 0.05	8.30 ± 0.34
Leucogranite GB (Holtz, F.) - 2	8.40 ± 0.6	n.d.	n.d.	1.62 ± 0.10	8.37 ± 0.69
Qu8N2 (melt inclusions)	11.0 ± 0.7†	272.0 ± 11	11.11 ± 0.45	1.96 ± 0.14	10.84 ± 1.07
Albite glass Ab83 (Behrens, H.)	11.71 ± 0.10	n.d.	n.d.	2.06 ± 0.03	11.62 ± 0.24
Albite glass Ab84 (Behrens, H.)	11.95 ± 0.12	n.d.	n.d.	2.07 ± 0.03	11.70 ± 0.24
Qu8N2 (melt inclusions)	13.1†	320.3 ± 16	13.06 ± 0.65	2.26 ± 0.08	13.24 ± 0.67
Qu8N2 (melt inclusions)	16.1 ± 0.6†	397.4 ± 2.5	16.17 ± 0.10	2.60 ± 0.04	16.20 ± 0.36

Notes: KF = Karl-Fischer method. n.d. = not determined. $I\left(\frac{3550\ cm^{-1}}{490\ cm^{-1}}\right)$ = Ratio of the integral intensity of the 3550 cm^{-1} and the 490 cm^{-1} bands.

Column 4: Amplitude method (method I): H_2O (wt%) = 0.0404 * A + 0.1296 (A – Amplitude); r^2 = 0.999; SD = 0.13; n = 18. Column 6: Integral intensity method (method II): H_2O (wt%) = 0.1642 + 3.239 * I + 1.127 * I^2; r^2 = 0.997; SD = 0.26; n = 27.

*****Analyzed by SIMS.

†Analyzed by EMPA = determined indirectly by subtracting the oxide sum (in wt%) of electron microprobe analysis from 100%.

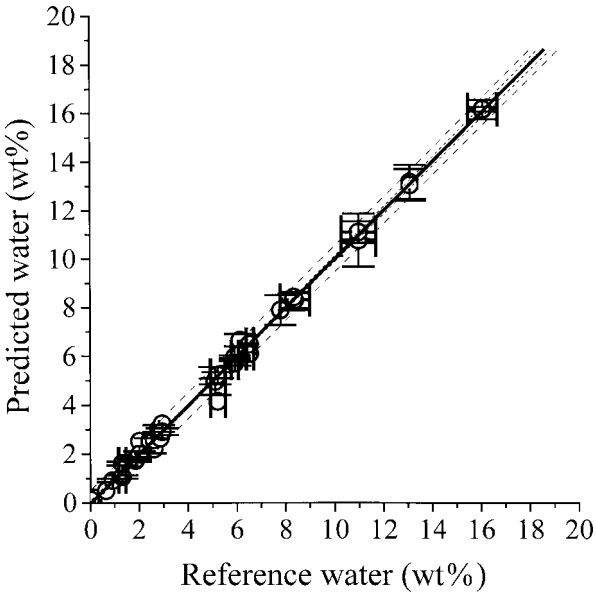

FIGURE 3. Reference water (X) vs. predicted water (Y), determined by confocal laser Raman microprobe spectroscopy (values in wt% H_2O). Prediction bands = dashed; confidence bands = short dashed.

minations were made. The other data points represent single measurements. The regression gives the following relationship between the concentration of water determined by KF, EMPA, and SIMS (X) and the H_2O concentration determined by Raman spectroscopy (Y):

$$Y\ (wt\%) = 0.99844 * X\ (wt\%) + 0.00539 \qquad (1)$$

Regression data: $r^2 = 0.99765$ SD = 0.21 n = 45

Where X is the reference water, Y is the predicted water, r is the correlation coefficient, SD is the standard deviation of the fit, and n is the number of data points.

The results indicate that Raman spectroscopy can be used for quantitative determination of water in granitic and pegmatitic silicate glasses in the range from 0 to 20 wt% H_2O. However, because the O-H stretching band envelope at 3550 cm^{-1} contains contributions from several hydrous species (e.g., OH, Si-OH, Al-OH, H_2O, etc), equivalent water concentrations are used.

Note that the electron microprobe totals (<84 wt%) for the melt inclusions containing 16 wt% H_2O are compatible with the Raman results for water in the glasses.

One test was provided by well-studied melt inclusions (Schmitt 1999) in quartz phenocrysts from rhyolites of the Purico Complex in the Central Andes. SIMS measurements have shown that some of the melt inclusions contain 4.0 ± 0.2 wt% H_2O. Raman spectroscopy of the identical inclusions gives values of 4.3 ± 0.4 wt%. The apparently larger scatter in values obtained by the Raman compared to the SIMS-method is the result of some inhomogenities of the H_2O-content in the studied inclusions. A slight zoning in the water content was often observed with somewhat higher concentrations in the inclusion center and lower values near the inclusion wall. This effect is seen only by the Raman-method which has superior spatial resolution (~2 μm) compared to the used SIMS analysis.

For a second test, the water contents of a large number (n = 319) of homogenized F-, P-, and B-rich silicate melt inclusions in a pegmatite quartz associated with the Variscan Ehrenfriedersdorf tin-granite in Saxony/East-Germany were determined. The melt inclusions were homogenized at temperatures between 500 to 800 °C at atmospheric pressure or at 1 kbar using conventional hydrothermal rapid-quench techniques (see also Thomas et al. 2000). After each run, the samples were quenched in liquid nitrogen with quenching rates of about 400 °C/s or isobarically in the case of the used rapid-quench technique. The results are arranged in 5 groups (Gauss peak fitting procedure, $r^2 = 0.9998$) and are given in Table 2. Group V represents with 21.5 ± 1.1 wt% (n = 21) the highest water concentration of totally homogenized melt inclusions in the studied pegmatite quartz (see Thomas and Webster 2000). The following Raman data were obtained:

$$\text{Amplitude } A = 538 \pm 26 \rightarrow 21.9 \pm 1.1 \text{ wt\% } H_2O \qquad \text{(Method I)}$$

$$I\left(\frac{3550\ cm^{-1}}{490\ cm^{-1}}\right) = 3.13 \pm 0.11 \rightarrow 21.3 \pm 1.2 \text{ wt\% } H_2O \qquad \text{(Method II)}$$

The water content of 21.5 wt% corresponds to the critical point (712 °C, 1 kbar) of the experimentally determined solvus boundary in the X_{H_2O}-T pseudobinary system of the Ehrenfriedersdorf pegmatite (see Thomas et al. 2000).

Representative EMP and SIMS analyses of melt inclusions in the pegmatite quartz are presented in Table 3. During the study of these extremely water-, F-, and P-rich melt inclusions (see also Thomas et al. 2000), it was observed that such water-rich glasses are not stable over long periods under the exciting laser radiation. This is also confirmed by heating experiments on unopened melt inclusions in quartz. At 400 °C, a rapid structural reorganization of the glass occurs as indicated by an irreversible and significant reduction of the band intensity at 3550 cm^{-1}, and by the appearance, after cooling, of a new sharp band centered at 3647 cm^{-1} (see Fig. 1). Measurement of the reduced 3550 cm^{-1} band in the heat treated samples is ineffective for

TABLE 2. Water contents of totally homogenized melt inclusions in pegmatite quartz Qu8 from Ehrenfriedersdorf using Raman spectrometry (method I)

Gaussian peak	Water content (wt%)	n
I	2.4 ± 0.9	52
II	6.4 ± 1.7	107
III	12.1 ± 1.7	115
IV	16.3 ± 1.6*	24
V	21.5 ± 1.1*	21

* Homogenized by rapid-quench hydrothermal experiments.

TABLE 3. Representative oxide and element concentrations (in wt%) in melt inclusions, homogenized at 650 and 1 kbar

	Melt A	Melt B
SiO_2	67.47 ± 1.09	37.98
TiO_2	0.02 ± 0.01	n.d.
SnO_2	0.10 ± 0.02	0.48
Al_2O_3	12.23 ± 0.52	8.74
B_2O_3	0.20 *	4.12
FeO	0.30 ± 0.05	1.27
MnO	0.04 ± 0.01	0.07
MgO	d.l.†	d.l.†
CaO	0.03 ± 0.01	d.l.†
Na_2O	3.35 ± 0.14	2.85
K_2O	3.15 ± 0.55	3.37
Rb_2O	0.44 ± 0.04	> 0.35
P_2O_5	1.52 ± 0.09	0.57
F	1.93 ± 0.37	2.60
Cl	0.15 ± 0.02	5.78
H_2O	9.80 ± 1.2	31.80
Sum	100.73	99.98
ASI‡	1.33	1.02

Notes: sample Qu8: fluorine-, boron-, and phosphorous rich pegmatite of the Varican Ehrenfriedersdorf tin-tungsten deposit of Saxony, Germany. Melt A and melt B represent two different types of melt inclusions simultaneously trapped on the solvus boundary of the silicate (+ fluorine + boron + phosphorous) – water system (see Thomas et al. 2000).
†Detection limit.
*Determined by ion microprobe (SIMS) at Woods Hole Oceanographic Institution, MA, U.S.A. by Jim Webster.
‡Molar aluminum saturation index.

the determination of water concentrations due to the formation of new water species and the destruction of others. Behrens (1995) has shown that simple drying at 105 °C can cause a significant loss of water from the sample for glasses with high water contents (≥7 wt%).

Except for the very rare case of fluorescence (e.g., the Macusani glass), the results suggest that confocal laser Raman spectrometry is a viable analytical technique for quantitative determination of the water content of silicate melt inclusions in the concentration range of 0 to 20 wt% H_2O.

The results of this study demonstrate that confocal laser Raman spectroscopy is a useful analytical technique for the study of the water contents of melt inclusions as small as 3 μm in diameter. Furthermore, with Raman spectroscopy one can investigate many melt inclusions in a relatively short time with a minimum of sample preparation—it is possible to analyze a single inclusion in less than 5 minutes. With further technological improvements the technique should become widely applicable, and so this method has the potential to become a useful, high-spatial resolution spectroscopic technique.

ACKNOWLEDGMENTS

I am grateful to H. Behrens and F. Holtz (University of Hannover), J.D. Webster (American Museum of Natural History, New York) as well as H.R. Westrich (Sandia National Laboratories, Albuquerque, New Mexico) for providing natural and synthetic glass samples for the calibration work. I thank W. Heinrich (GFZ Potsdam) for performing some hydrothermal rapid quench experiments to obtain some extremely water-rich and homogeneous melt inclusions of pegmatite composition. I thank also A. Schmitt (GFZ Potsdam) for some well characterized melt inclusions in quartz and plagioclase from ignimbrites of the Central Andes.

I thank J.D. Webster, W. Heinrich, and M. Wiedenbeck for their help in the preparation of this manuscript. The manuscript benefited particularly from critical remarks by two anonymous reviewers. Alan J. Anderson (Antigonish, Nova Scotia, Canada) helped extensively to streamline and focus the presentation.

REFERENCES CITED

Behrens, H. (1995) Determination of water solubilities in high-viscosity melts: An experimental study on $NaAlSi_3O_8$ and $KAlSi_3O_8$ melts. European Journal of Mineralogy, 7, 905–920.

Chabiron, A., Pfeifert, C., Pironon, J., and Cuney, M. (1999) Determination of water content in melt inclusions by Raman spectrometry. In : H. Ristedt, Managing Editor; V. Lüders, R. Thomas, and A. Schmidt-Mumm, Guest Editors, Terra Nostra–Schriften der Alfred-Wegner-Stiftung 99/6; ECROFI XV (European Current Research On Fluid Inclusions), Abstracts and Program, June 21–24, 1999, p. 68–69. GeoForschungsZentrum Potsdam.

Cooney, T.F., Wang, L., Sharma, S.K., Gauldie, R.W., and Montana, A.J. (1994) Raman spectral study of solid and dissolved poly(vinyl alcohol) and ethylene-vinyl alcohol copolymer. Journal of Polymer Science: Part B: Polymer Physics, 32, 1163–1174.

Ihinger, P.D., Hervig, R.L., and McMillan, P.F. (1994) Analytical methods for volatiles in glasses. In Mineralogical Society of America Reviews in Mineralogy, 30, Chapter 2, 67–121.

Matson, D.W., Sharma, S.K, and Philpotts, J.A. (1986) Raman spectra of some tectosilicates and of glasses along the orthoclase-anorthite and nepheline-anorthite joins. American Mineralogist, 71, 694–704.

McMillan P.F. (1994) Water solubility and speciation models. In Mineralogical Society of America Reviews in Mineralogy, 30, Chapter 4, 131–156.

McMillan, P.F. and Hofmeister, A.M. (1988) Infrared and Raman spectroscopy. In Mineralogical Society of America Reviews in Mineralogy, 18, Chapter 4, p. 99–159.

Mysen, B.O., Holtz, F., Pichavant, M., Beny, J.-M., and Montel, J.-M. (1997) Solution mechanisms of phosphorus in quenched hydrous and anhydrous granitic glass as function of the peraluminosity. Geochimica et Cosmochimica Acta, 61, 3913–3926.

Pandya, N., Muenow, D.W., and Sharma, S.K. (1992) The effect of bulk composition on the speciation of water in submarine volcanic glasses. Geochimica et Cosmochimica Acta, 56, 1875–1883.

Roedder E. (1984) Fluid inclusions. In Mineralogical Society of America Reviews in Mineralogy, 12, 644.

Schmitt, A. (1999) Melt generation and magma chamber processes in the Purico Complex and implications for ignimbrite formation in the Central Andes. Unpublished Ph.D. Thesis, University Giesen, Germany, 107 p.

Sharma, S.K, Cooney, T.F., Wang, Z., and van der Laan, S. (1997) Raman band assignments of silicate and germanate glasses using high-pressure and high-temperature spectral data. Journal of Raman Spectroscopy, 28, 697–709.

Stolper, E. (1982) Water in silicate glasses: an infrared spectroscopic study. Contribution to Mineralogy and Petrology, 81, 1–17.

Thomas, R. and Klemm, W. (1997) Microthermometric study of silicate melt inclusions in Variscan granites from SE Germany: Volatile contents and entrapment conditions. Journal of Petrology, 38, 1753–1765.

Thomas, R. and Webster, J.D. (2000) Strong tin enrichment in a pegmatite-forming melt. Mineralium Deposita, in press.

Thomas, R., Webster, J.D., and Heinrich, W. (2000): Melt inclusions in pegmatite quartz: Complete miscibility between silicate melts and hydrous fluids at low pressure. Contribution to Mineralogy and Petrology (in press).

MANUSCRIPT RECEIVED SEPTEMBER 15, 1999
MANUSCRIPT ACCEPTED FEBRUARY 1, 2000
PAPER HANDLED BY ANNE M. HOFMEISTER